Acta Crystallographica Section D
Biological Crystallography
ISSN 1399-0047

Neutron structure of the cyclic glucose-bound xylose isomerase E186Q mutant

Parthapratim Munshi,[a,b]‡ Edward H. Snell,[c] Mark J. van der Woerd,[d] Russell A. Judge,[e] Dean A. A. Myles,[a] Zhong Ren[f] and Flora Meilleur[a,g]*

[a]Neutron Sciences Directorate, Oak Ridge National Laboratory, Oak Ridge, TN 37831, USA, [b]Department of Chemistry, Middle Tennessee State University, Murfreesboro, TN 37132, USA, [c]Department of Structural Biology, SUNY Buffalo, Hauptman–Woodward Medical Research Institute, Buffalo, NY 14203, USA, [d]Department of Biochemistry and Molecular Biology, Colorado State University, Fort Collins, CO 80523, USA, [e]Structural Biology, AbbVie Inc., North Chicago, IL 60064, USA, [f]Renz Research Inc., Westmont, IL 60559, USA, and [g]Department of Molecular and Structural Biochemistry, North Carolina State University, Raleigh, NC 27695, USA

‡ Current address: Chemistry Department & Center for Informatics, School of Natural Sciences, Shiv Nadar University, Dadri, UP 203207, India.

Correspondence e-mail: flora_meilleur@ncsu.edu

Received 12 September 2013
Accepted 28 October 2013

PDB reference: cyclic glucose-bound xylose isomerase, 4lnc

Ketol-isomerases catalyze the reversible isomerization between aldoses and ketoses. D-Xylose isomerase carries out the first reaction in the catabolism of D-xylose, but is also able to convert D-glucose to D-fructose. The first step of the reaction is an enzyme-catalyzed ring opening of the cyclic substrate. The active-site amino-acid acid/base pair involved in ring opening has long been investigated and several models have been proposed. Here, the structure of the xylose isomerase E186Q mutant with cyclic glucose bound at the active site, refined against joint X-ray and neutron diffraction data, is reported. Detailed analysis of the hydrogen-bond networks at the active site of the enzyme suggests that His54, which is doubly protonated, is poised to protonate the glucose O5 position, while Lys289, which is neutral, promotes deprotonation of the glucose O1H hydroxyl group *via* an activated water molecule. The structure also reveals an extended hydrogen-bonding network that connects the conserved residues Lys289 and Lys183 through three structurally conserved water molecules and residue 186, which is a glutamic acid to glutamine mutation.

1. Introduction

D-Xylose ketol-isomerase (XI; EC 5.3.1.5) catalyzes the isomerization of aldose and ketose sugars in some bacteria and fungi. XI is used industrially on a large scale to isomerize glucose to fructose, a sweetener used extensively in the food industry, and in biotechnology to convert biomass into biofuels and into high-end biochemical reagents. The design of XI enzymes with improved performance (activity, specificity and thermal stability) is of interest to reduce process costs by allowing more favorable chemical reaction environments (different optimal pH and temperature) and/or to re-engineer the enzyme to produce biochemical products of choice. In efforts to engineer an enzyme with a pH optimum below the alkaline range typical of most wild-type XIs, Van Tilbeurgh *et al.* (1992) reported an E186Q mutant of the XI from *Actinoplanes missouriensis* that is most active in a form with Mn^{2+} bound and has a drastically shifted pH optimum of 6.2. Here, we investigate the neutron crystallographic structure of the E186Q mutant of D-xylose isomerase from *Streptomyces rubiginosus*, a homotetramer with 43 kDa subunits which is perhaps the best studied of the XI enzymes, with the intention of further characterizing its mechanism.

The linearization and reversible isomerization of D-xylose or D-glucose by XI enzymes are thought to be ruled by a complex metal-ion-catalyzed reaction that proceeds through a hydride-transfer mechanism. The active site contains two divalent metal cations. Wild-type XI shows good catalytic

activity with either Mg^{2+}, Co^{2+} or Mn^{2+} bound. Numerous structural, mutational, computational, metal-binding and biochemical studies have shown that the active site is highly conserved in XI between different species and that ligand binding results in similar metal cofactor movement and related conformational changes through the reaction (Allen *et al.*, 1994; Carrell *et al.*, 1989, 1994; Cha *et al.*, 1994; Collyer *et al.*, 1990; Fenn *et al.*, 2004; Jenkins *et al.*, 1992; Lambeir *et al.*, 1992; Lavie *et al.*, 1994; van Tilbeurgh *et al.*, 1992; Whitaker *et al.*, 1995; Whitlow *et al.*, 1991). These studies have provided a consensus model for the catalytic reaction, in which His54 is implicated in the binding and linearization of the cyclic sugar and Lys183 is thought to be involved in the binding of the extended sugar conformation. Biochemical data have shown that mutation of His54 to Asn or Gln only slows the reaction mechanism (Lee *et al.*, 1990; Whitaker *et al.*, 1995), while mutating Lys183 to Ser, Gln or Arg results in a total loss of activity (Lambeir *et al.*, 1992). Key questions remain on the precise nature and detail of the steps that are involved in the linearization of the cyclic substrate.

Early X-ray diffraction studies led to suggestions that His54, assisted by Asp57, acts as a base in the ring-opening step of the reaction (Collyer *et al.*, 1990; Whitlow *et al.*, 1991). In this model, His54 accepts a proton from the O1 hydroxyl group of the sugar and transfers it to the O5 position. The sugar ring opens only after the proton starts moving from NE2 of His54 towards O5 of the sugar. The approach of Asp57 towards His54, which enhances the basicity of the histidine side chain, initiates ring opening (Asbóth & Náray-Szabó, 2000). Analysis of steric constraints and active-site geometry in a 0.95 Å resolution X-ray structure of cyclic glucose-bound XI led Fenn *et al.* (2004) to propose an alternate mechanism, in which His54 acts as an acid, donating a proton to the glucose O5 atom. Deprotonation of the O1H hydroxyl group then occurs through activated water molecules involved in hydrogen-bonding interactions with Asp57. In addition, Fenn *et al.* (2004) noted that the proximity of Lys289 could offer an alternative base and pathway, but they postulated that the pK_a would be too high to permit sufficient base catalysis under the crystallization conditions used.

More recently, a series of neutron diffraction studies on different metal-bound and ligand-bound states have provided additional information on the protonation and hydration state of the enzyme in its ligand-free (Katz *et al.*, 2006; Meilleur *et al.*, 2006), substrate-bound (Kovalevsky *et al.*, 2010), inhibitor-bound (Kovalevsky *et al.*, 2012) and product-bound (Kovalevsky *et al.*, 2008) forms. Neutron diffraction offers a distinct advantage over X-ray diffraction in being able to more readily locate H atoms (or their D isotopes) in crystallographic structures. This is because H or D atoms scatter neutrons with a similar magnitude as C, N and O atoms. In contrast, H or D atoms, with just one electron, scatter X-rays only weakly and are difficult if not impossible to locate in more mobile regions of a protein, even when data are available to ultrahigh resolution. The neutron studies have enabled the charge state of key catalytic residues to be examined at several steps along the reaction pathway in wild-type XI crystals and refocused attention on the potential role of Lys289 in the catalytic mechanism (Kovalevsky *et al.*, 2010).

Here, we extend these analyses by reporting the first neutron diffraction structure of the E186Q mutant of *S. rubiginosus* D-xylose isomerase in which cyclic D-glucose substrate is bound at the active site of the Mn^{2+} metal form of the enzyme (labeled E186Q-Mn-Glc). While Glu186 is not directly involved in metal binding, it is sufficiently close to the active site to interfere with binding and catalysis in XI (van Tilbeurgh *et al.*, 1992). Our E186Q-Mn-Glc mutant structure is consistent with a model for ring opening and sugar linearization through the action of His54, which is doubly protonated, acting as an acid to protonate the glucose O5 position. Our structure further suggests that linearization is assisted by Lys289, which is neutral, acting as a proton acceptor in the deprotonation of the O1H glucose hydroxyl group. Residue 186 is positioned to contribute to an intricate hydrogen-bonding network between Lys289 and Lys183, and could promote proton abstraction from the O1 hydroxyl group of the bound cyclic substrate through Lys289, which is neutral in our structure and which has been shown to be essential for catalysis (Kovalevsky *et al.*, 2010).

2. Materials and methods

2.1. Crystallization

D-Xylose isomerase E186Q mutant enzyme supplied by Genencor International (Palo Alto, California, USA) was purified and crystallized at pH 7.7 in deuterated solvent as described previously (Meilleur *et al.*, 2006; Snell *et al.*, 2006). The xylose isomerase with glucose bound was prepared as described by Fenn *et al.* (2004). A crystal of approximately 8 mm^3 was soaked in an increasing concentration (up to 600 m*M*) of hydrogenated α-D-glucose in artificial deuterated mother liquor over a period of a week. The crystal was then mounted in a 5 mm diameter quartz capillary.

2.2. Data collection

Neutron quasi-Laue diffraction data were collected at room temperature on the LADI-I beamline installed at end-station T17 of cold neutron guide H142 at Institut Laue–Langevin (ILL; Cipriani *et al.*, 1996; Myles *et al.*, 1997). An Ni/Ti multilayer wavelength selector was used to select a narrow band pass ($d\lambda/\lambda \simeq 25\%$) tuned to a wavelength range of 3.6–5.0 Å in order to reduce the number of spatially overlapped reflections at the detector (Meilleur *et al.*, 2006). Data were collected from two crystal orientations to help to fill the blind region and therefore increase the completeness. A total of 27 images of 24 h exposure each were collected. Each image covers approximately 8° of reciprocal space. Following neutron data collection, an X-ray data set was collected at room temperature from the same crystal for joint X-ray and neutron refinement. X-ray data were recorded on a MAR Research 345 mm image-plate detector using a rotating-anode X-ray generator with a copper target (λ = 1.54 Å).

2.3. Data reduction

Neutron Laue data were processed using the *Precognition* software package (Renz Research Inc., Westmont, Illinois, USA), which was modified for neutron diffraction and to account for the cylindrical geometry of the detector. *Precognition* was originally designed to deconvolute spatially overlapping reflections in X-ray Laue diffraction images. Following integration, the data were wavelength-normalized using *LSCALE* (Arzt *et al.*, 1999) and then scaled and merged using *SCALA* (Winn *et al.*, 2011). X-ray data were indexed and integrated with *MOSFLM* (Leslie & Powell, 2007) and then scaled and merged using *SCALA*.

2.4. Refinement

The room-temperature X-ray structure of the D-xylose isomerase E186Q mutant with α-glucose bound was refined with *phenix.refine* (Adams *et al.*, 2002) starting from an ultrahigh-resolution (0.84 Å) model of the substrate-free enzyme from which water molecules had been removed (E. H. Snell, unpublished results). Following initial rigid-body optimization, individual coordinates, isotropic B factors and occupancies were refined, followed by an automatic ordered solvent (water) update (picking/removing) and checks of the model in electron density ($F_{obs} - F_{calc}$ and $2F_{obs} - F_{calc}$ maps) using *Coot* (Emsley & Cowtan, 2004). Metal ions were located at sites M1 and M2 and refined. The difference $F_{obs} - F_{calc}$ map showed significant density for a cyclic glucose molecule at the active site, which was fitted to the electron density using the *LigandFit* wizard (Terwilliger *et al.*, 2007).

Joint X-ray and neutron refinement (XN) was performed with *phenix.refine* using the room-temperature X-ray structure (1.8 Å) as a starting model. H atoms and exchangeable H/D atoms were added to the structure using the *phenix.ready_set* command-line tool. R_{free} flags that are consistent with both the X-ray and neutron data sets were generated using *phenix.refine*. Rigid-body optimization was followed by positional, atomic displacement and occupancy parameter refinement. The protonation states of histidine, lysine, aspartate and glutamate residues were determined by inspection of $2F_{obs} - F_{calc}$ and $F_{obs} - F_{calc}$ neutron scattering density maps and the occupancies of respective H/D atoms were refined. D atoms were added to water O atom positions identified from the X-ray structure and the atomic positions and isotropic B factors of D_2O water molecules were refined. Water molecules that showed negative $F_{obs} - F_{calc}$ or no $2F_{obs} - F_{calc}$ neutron scattering density maps were removed.

3. Results

X-ray and neutron data-reduction statistics are summarized in Table 1. Initial predictions in *LAUEGEN* suggested that more than 25% of reflections would be spatially overlapped at the detector. Integration using the *Precognition* software package enabled a substantial fraction of these spatially overlapped reflections to be recovered. It is notable that the final neutron data set is 93% complete at 2.2 Å resolution.

Table 1
X-ray and neutron diffraction data-collection and reduction statistics.

Values in parentheses are for the highest resolution shell.

	X-ray	Neutron
Source	Rotating anode	LADI-I, ILL
Space group	*I*222	
Unit-cell parameters (Å)	a = 93.97, b = 99.52, c = 102.92	
Resolution (Å)	25.00–1.83 (1.92–1.83)	40.86–2.17 (2.29–2.17)
No. of observed reflections	86387 (8287)	155063 (6001)
No. of unique reflections	35317 (3975)	23398 (2397)
Multiplicity	2.4 (2.1)	6.6 (2.5)
Completeness (%)	83.2 (64.6)	93.0 (66.7)
$R_{p.i.m.}$ (%)	11.9 (21.1)	10.8 (13.9)
Wavelength (Å)	1.54	3.6–5.0
Mean $I/\sigma(I)$	4.3 (3.4)	11.7 (3.5)

Table 2
Model-refinement statistics based on joint X-ray and neutron scattering data.

R_{work}†	15.04 (X)/28.44 (N)
R_{free}†	20.89 (X)/32.19 (N)
No. of atoms	
Protein	3027
Glucose	12
Metal ions	3
Water O	289
R.m.s.d., bond lengths (Å)	0.022
R.m.s.d., angles (°)	2.136
Mean B factors (Å^2)	
Protein	21.45
Glucose	27.29
Mn	25.91
Mg/Mn	17.58
Water	32.02

† X and N stand for X-ray and neutron, respectively.

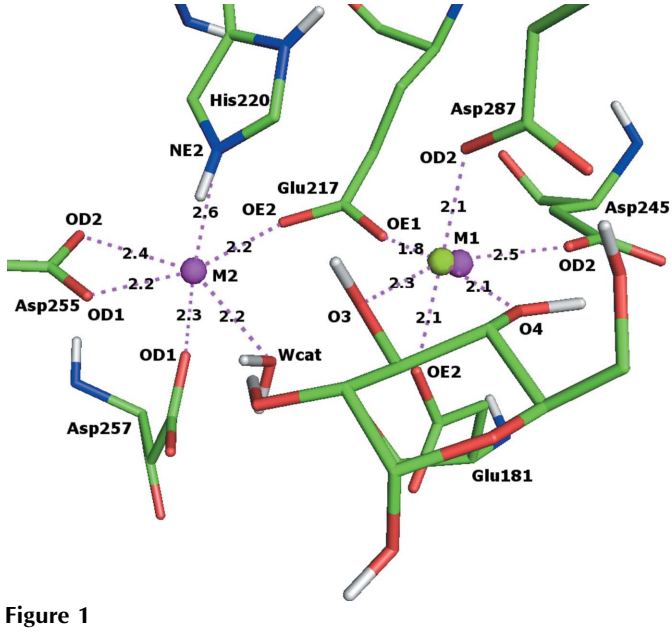

Figure 1
Metal-ion coordination at the active site of cyclic D-glucose-bound E186Q xylose isomerase. The structural metal site, M1, is modeled as two metal ions, Mg^{2+} and Mn^{2+}, with occupancies of 75 and 25%, respectively. The catalytic metal site, M2, is fully occupied by Mn^{2+}. Both M1 and M2 have a coordination number of six, forming an octahedral geometry. Distances are given in Å. D but not H atoms are shown for figure clarity. Mn^{2+}, magenta; Mg^{2+}, green.

The X-ray and neutron (X/N) refinement statistics for the final structure are summarized in Table 2. The $2F_{obs} - F_{calc}$ electron-density map shows the partially deuterated cyclic α-glucose bound at the active site of the enzyme (Figs. 1 and 2*a*). Both metal cation sites have high occupancy, with electron-density peaks of 24σ at the structural M1 metal site and 30σ at the catalytic M2 metal site. The electron density is consistent with an Mn^{2+} ion at M1 with a partial occupancy of ∼75%. We note that this could also be modeled as two metal ions, Mg^{2+} and Mn^{2+}, with occupancies of 75 and 25%, respectively. The catalytic metal site, M2, is fully occupied by Mn^{2+}. Both M1 and M2 have coordination number six, forming an octahedral geometry (Fig. 1). Superposition and comparison of the neutron and X-ray models show that the metal ions cannot be visualized in the neutron maps. This is not surprising, because metal ions scatter neutrons much more weakly than they scatter X-rays, and the neutron scattering length of a single Mg (5.375 fm) or Mn (−3.73 fm) atom is similar to that of a single D (6.61 fm) or H (−3.74 fm) atom.

The active-site hydrogen-bond network along with the density maps is shown in Fig. 3. The catalytic water W_{cat} is clearly present as a DOD molecule. Careful inspection of the neutron structure suggests that none of the active-site carboxylic acid groups (Glu181, Glu217, Asp245, Asp255, Asp257 and Asp287) are protonated. The structural metal ion M1 is coordinated by O3 and O4 of glucose, OD2 of Asp245, OE1 of Glu217, OD2 of Asp287 and OE2 of Glu181. The catalytic metal ion M2 is coordinated by O of the catalytic water W_{cat}, OE2 of Glu217, OD2 and OD1 of Asp255, NE2 of His220 and OD1 of Asp257. Surprisingly, His220 appears to be doubly protonated in our E186Q-Mn-Glc structure. This suggests that the coordination between NE2 of His220 and M2 is weak, which may influence the electrostatic potential of the catalytic metal ion in the E186Q mutant.

The D-glucose substrate is bound in the cyclic form (Fig. 2*a*). The O4 hydroxyl group forms a strong hydrogen bond to OE1 of Glu181 (O···O = 2.58 Å and ∠O—D···O = 127.1°). The O3 hydroxyl is hydrogen bonded to the catalytic water W_{cat} (DOD 255 in the PDB deposition) and to another water molecule W1 (DOD 81 in the PDB deposition). Water W1 is tightly placed at the active site, forming two more N—D···O hydrogen bonds to the doubly protonated His220 and the positively charged Lys183 (Fig. 2*b*) and an additional O—D···O hydrogen bond to the O2 hydroxyl group of the cyclic glucose. The other two protons of Lys183 are hydrogen-bonded to the main-chain carbonyl O atom and the OE1 atom of Gln186, respectively. The O1 atom of cyclic D-glucose forms a hydrogen bond to water molecule W2 (DOD 114 in the PDB deposition). The ring O5 of the cyclic D-glucose forms a strong (O···N = 2.72 Å and ∠O—D···O = 156.0°) hydrogen bond to the proton at NE2 of the doubly protonated His54; the other proton at ND1 is hydrogen-bonded to the carboxylate OD2 atom of Asp57. Water W3 (DOD 109 in the PDB deposition), which interacts weakly (O···O = 3.02 Å and ∠O—D···O = 86.8°) with Asp57, is not within hydrogen-bonding distance of the O1 hydroxyl group of the cyclic glucose (O···O = 4.69 Å).

The Lys289 amino group is best modeled as neutral in our structure (Fig. 2*c*), with the $-ND_2$ group pointing towards the active site (Figs. 3 and 4) to form a strong hydrogen bond (O···O = 2.50 Å, ∠O—D···N = 97.0°) to water W2 and a weaker (N···O = 3.45 Å, ∠O—D···N = 105.6°) hydrogen bond to water W4 (DOD 113 in the PDB deposition). The neutron maps show a well defined and intricate hydrogen-bond network that extends from the neutral $-ND_2$ group of

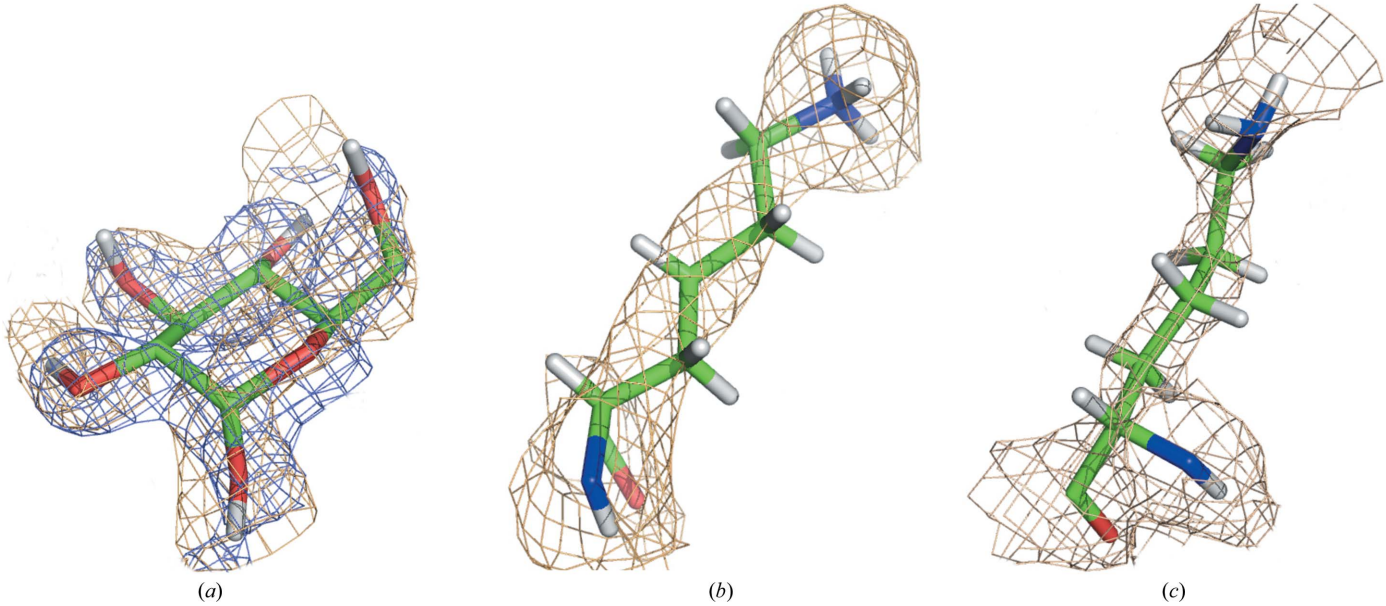

Figure 2
(*a*) Superposition of the X-ray $2F_{obs} - F_{calc}$ density map (blue) contoured at 2.0σ and the neutron scattering $2F_{obs} - F_{calc}$ density map (light orange) contoured at 1.5σ for the cyclic glucose moiety. (*b*) The neutron scattering $2F_{obs} - F_{calc}$ density map contoured at 2.5σ for charged Lys183. (*c*) The neutron scattering $2F_{obs} - F_{calc}$ density map contoured at 2.0σ for neutral Lys289.

Lys289 to the charged $-ND_3^+$ group of Lys183 through waters W4 and W5 (DOD 69 in the PDB deposition), with the latter forming a hydrogen bond to water W4 and atom OE1 of Gln186, and with Gln186 forming two hydrogen bonds through atom OE1 and the main-chain carbonyl O atom to Lys183 DZ1 and DZ3, respectively.

A total of 309 water O atoms were located using $F_{obs} - F_{calc}$ electron-density maps. In the subsequent X/N refinement, a total of 289 water molecules were located, of which ten were modeled as O atoms, six as OD ions and 273 as complete DOD molecules. It is worth noting that all 273 D_2O molecules refined in this structure are oriented to form appropriate hydrogen bonds to neighboring residues, water molecules, bound substrate and the metal ions.

4. Discussion

The active site of XI is highly conserved throughout all of the organisms studied and few differences were expected between the overall structure of our *S. rubiginosus* E186Q-Mn-Glc and the other wild-type X-ray structures of cyclic glucose-bound D-xylose isomerase (PDB entries 1s5m and 1xib; Fenn *et al.*, 2004; Carrell *et al.*, 1994). However, the addition of H and D atoms provides a more complete understanding of the protonation and hydration state of the E186Q-Mn-Glc structure, and we find that under the conditions of our experiment (i) the glucose molecule is bound in the cyclic form, (ii) His54 is doubly protonated, (iii) His220 is doubly protonated, (iv) Lys289 is neutral, (v) Lys183 is charged and (vi) Gln186 is involved in an intricate hydrogen-bonding network that bridges between Lys289 and Lys183 (Fig. 3).

These results are consistent in part with earlier models for ring opening and sugar linearization through the action of His54, which is doubly protonated, as an acid to protonate the glucose O5 position. Linearization also requires concerted deprotonation of the O1 hydroxyl group by an active-site base. Fenn *et al.* (2004) suggested that this could be carried out by a catalytic water molecule that is activated by Asp57 through an extended pathway that involves two water molecules (HOH 2283 and HOH 2119 in PDB entry 1s5m). However, only one of these waters, HOH 2119, is clearly visible in our E186Q-Mn-Glc neutron structure (W3 in Fig. 3, DOD 109 in the PDB deposition), while X-ray density near HOH 2283 is ambiguous. Conversely, Kovalevsky *et al.* (2012) observed only HOH 2283 in their XI-WT-Cd-Glu neutron structure, while HOH 2119 was absent. These model-dependent observations are inconsistent with a water-activation pathway involving Asp57.

In their earlier work, Fenn *et al.* (2004) noted that the proximity of Lys289 to the O1 hydroxyl could provide an alternative base and pathway for deprotonation, although they questioned whether the pK_a and inherent disorder would support base catalysis. It is therefore interesting that in our E186Q-Mn-Glc neutron structure the side-chain density of Lys289 is best modeled as a neutral $-ND_2$ group (Figs. 2*c* and 3). This is consistent with previous neutron observations of Lys289 in the apo and cyclic glucose-bound forms of wild-type XI (Kovalevsky *et al.*, 2010). Moreover, in our E186Q-Mn-Glc structure Lys289 is positioned to act as a base to deprotonate the O1 hydroxyl group *via* an activated water molecule that is conserved (DOD 114 or W2 in our work, HOH 2217 in PDB entry 1s5m, DOD 1105 in PDB entry 3kcl) among the structures of cyclic glucose-bound xylose isomerase crystallized at pH 7.7 (Figs. 3 and 4).

Further supporting this putative role of Lys289 is the fact that its side chain has been observed pointing 'in' (towards the substrate) and 'out' (away from the substrate) in the neutron structures of wild-type XI (Kovalevsky *et al.*, 2010; PDB entry 3kcl). In both the 'in' and the 'out' conformations, Lys289 is hydrogen-bonded to Glu186 through two conserved water molecules, W4 (DOD 113 in the PDB deposition, HOH 2306 in PDB entry 1s5m, DOD 1084 in PDB entry 3kcl) and W5 (DOD 69 in the PDB deposition, HOH 2064 in PDB entry 1s5m, DOD 1067 in PDB entry 3kcl), suggesting a

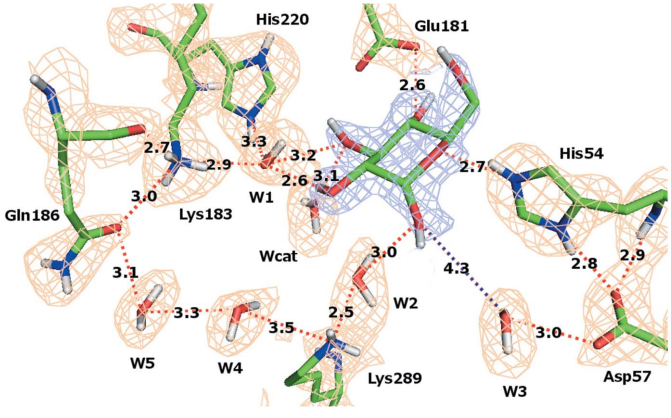

Figure 3
Cyclic D-glucose bound to the E186Q mutant of D-xylose isomerase. Hydrogen bonds are shown as red dashed lines. W3 and cyclic D-glucose O1H are not within hydrogen-bonding distance (blue dashed line). Distances are given in Å. D but not H atoms are shown for figure clarity. The X-ray $2F_{obs} - F_{calc}$ density map (blue) is contoured at 2.0σ; the neutron scattering $2F_{obs} - F_{calc}$ density map (light orange) is contoured at 2.5σ.

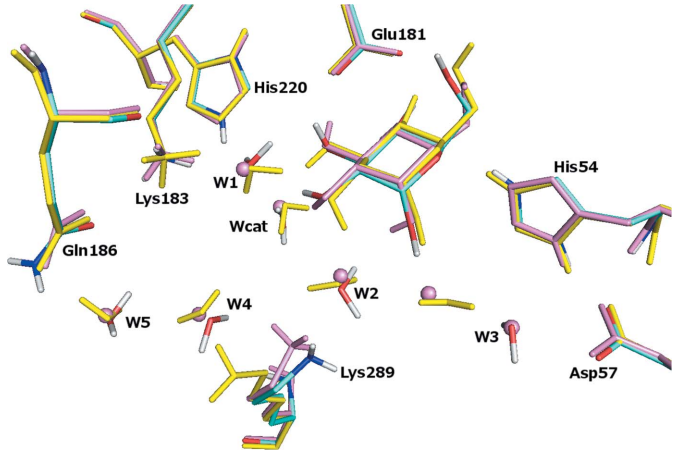

Figure 4
Xylose isomerase active sites from three cyclic glucose-bound structures. D but not H atoms are shown for figure clarity. Residues and water molecules are labeled for this work (see text for details). Cyan, this work; pink, PDB entry 1s5m; yellow, PDB entry 3kcl.

chaperoning role of the wild-type Glu186 residue in the conformation and protonation state of Lys289. Residue 186 also forms two hydrogen bonds to the charged $-ND_3^+$ group of the catalytically critical Lys183 residue in our E186Q-Mn-Glc structure and in wild-type structures. These data suggest that interactions of residue 186 with Lys183 may be important for Lys183 to adopt the required conformation to stabilize the linear sugar. Stabilizing interactions similar to those that we observe here between Glu186 and catalytic residues have frequently been observed in catalysis (Holliday *et al.*, 2009).

While most wild-type XI enzymes have a pH optimum of 8.5, van Tilbeurgh *et al.* (1992) reported that the E186Q mutant of D-xylose isomerase from *A. missouriensis* is most active with Mn^{2+} bound and has a pH optimum that is shifted to pH 6.2. Substitution of a negatively charged residue with a neutral one is expected to give rise to a net increase in positive charge within a $\sim$10 Å radius of the metal ions. In our *S. rubiginosus* E186Q-Mn-Glc structure, the mutated Gln186 residue is 6.4 Å away from the catalytic metal site M2. Although residue 186 does not bind directly to either metal ion, it forms a hydrogen bond to the main-chain >ND group of Asp255, a catalytic M2 metal ligand that is known to adopt alternate conformations in the substrate-bound and product-bound forms (Whitlow *et al.*, 1991; Fenn *et al.*, 2004). Removal of the negative charge in E186Q is likely to increase the metal affinity at M2 by lowering the pK_a of Asp255 (van Tilbeurgh *et al.*, 1992). The fact that His220 appears doubly protonated in E186Q-Mn-Glc suggests that the coordination between NE2 of His220 and M2 is weak, which may further influence the electrostatic potential of the catalytic metal ion.

Finally, we note that the E186Q-Mn-Glc crystals used in this study were grown and soaked in cyclic glucose solution at pH 7.7, in which the activity of the E186Q mutant enzyme is expected to be low, and we observed the expected cyclic α-glucose substrate form in the structure. Additional neutron diffraction experiments are under way to investigate the impact of lower pH on the micro-environment at the active site of the E186Q enzyme.

5. Conclusion

Sugar linearization at the active site of XI requires concerted protonation at position O5 and deprotonation of the O1 hydroxyl group. Our results on E186Q-Mn-Glc show that His54 is doubly protonated and is poised to act as the active-site acid. Lys289 is neutral in our structure and is able to act as a base to deprotonate the O1 hydroxyl group *via* an activated water molecule. The improved activity and lower pH optimum of E186Q XI has previously been discussed only in the context of metal affinity and isomerization. Our neutron analysis of E186Q-Mn-Glc extends this discussion to the linearization step by defining an intricate hydrogen-bond network that extends from the substrate O1 hydroxyl group through the neutral $-ND_2$ group of Lys289 and to the charged $-ND_3^+$ group of Lys183 which is essential for catalysis.

We thank Genencor International for providing the xylose isomerase. PM is supported by an award from the National Science Foundation (Award 0922719) to FM. We thank Pavel Afonine from Lawrence Berkeley National Laboratory for his instruction and help with *phenix.refine*. This research was sponsored in part by the Laboratory Directed Research and Development Program of Oak Ridge National Laboratory, which is managed by UT-Battelle LLC for the US Department of Energy under contract No. DO-AC05-00OR22725.

References

Adams, P. D., Grosse-Kunstleve, R. W., Hung, L.-W., Ioerger, T. R., McCoy, A. J., Moriarty, N. W., Read, R. J., Sacchettini, J. C., Sauter, N. K. & Terwilliger, T. C. (2002). *Acta Cryst.* D**58**, 1948–1954.

Allen, K. N., Lavie, A., Glasfeld, A., Tanada, T. N., Gerrity, D. P., Carlson, S. C., Farber, G. K., Petsko, G. A. & Ringe, D. (1994). *Biochemistry*, **33**, 1488–1494.

Arzt, S., Campbell, J. W., Harding, M. M., Hao, Q. & Helliwell, J. R. (1999). *J. Appl. Cryst.* **32**, 554–562.

Asbóth, B. & Náray-Szabó, G. (2000). *Curr. Protein Pept. Sci.* **1**, 237–254.

Carrell, H. L., Glusker, J. P., Burger, V., Manfre, F., Tritsch, D. & Biellmann, J. F. (1989). *Proc. Natl Acad. Sci. USA*, **86**, 4440–4444.

Carrell, H. L., Hoier, H. & Glusker, J. P. (1994). *Acta Cryst.* D**50**, 113–123.

Cha, J., Cho, Y., Whitaker, R. D., Carrell, H. L., Glusker, J. P., Karplus, P. A. & Batt, C. A. (1994). *J. Biol. Chem.* **269**, 2687–2694.

Cipriani, F., Castagna, J. C., Wilkinson, C., Lehmann, M. S. & Büldt, G. (1996). *Basic Life Sci.* **64**, 423–431.

Collyer, C. A., Henrick, K. & Blow, D. M. (1990). *J. Mol. Biol.* **212**, 211–235.

Emsley, P. & Cowtan, K. (2004). *Acta Cryst.* D**60**, 2126–2132.

Fenn, T. D., Ringe, D. & Petsko, G. A. (2004). *Biochemistry*, **43**, 6464–6474.

Holliday, G. L., Mitchell, J. B. O. & Thornton, J. M. (2009). *J. Mol. Biol.* **390**, 560–577.

Jenkins, J., Janin, J., Rey, F., Chiadmi, M., van Tilbeurgh, H., Lasters, I., De Maeyer, M., Van Belle, D., Wodak, S. J., Lauwereys, M., Stanssens, P., Mrabet, N. T., Snauwaert, J., Matthyssens, G. & Lambeir, A.-M. (1992). *Biochemistry*, **31**, 5449–5458.

Katz, A. K., Li, X., Carrell, H. L., Hanson, B. L., Langan, P., Coates, L., Schoenborn, B. P., Glusker, J. P. & Bunick, G. J. (2006). *Proc. Natl Acad. Sci. USA*, **103**, 8342–8347.

Kovalevsky, A. Y., Hanson, L., Fisher, S. Z., Mustyakimov, M., Mason, S. A., Forsyth, V. T., Blakeley, M. P., Keen, D. A., Wagner, T., Carrell, H. L., Katz, A. K., Glusker, J. P. & Langan, P. (2010). *Structure*, **18**, 688–699.

Kovalevsky, A., Hanson, B. L., Mason, S. A., Forsyth, V. T., Fisher, Z., Mustyakimov, M., Blakeley, M. P., Keen, D. A. & Langan, P. (2012). *Acta Cryst.* D**68**, 1201–1206.

Kovalevsky, A. Y., Katz, A. K., Carrell, H. L., Hanson, L., Mustyakimov, M., Fisher, S. Z., Coates, L., Schoenborn, B. P., Bunick, G. J., Glusker, J. P. & Langan, P. (2008). *Biochemistry*, **47**, 7595–7597.

Lambeir, A. M., Lauwereys, M., Stanssens, P., Mrabet, N. T., Snauwaert, J., van Tilbeurgh, H., Matthyssens, G., Lasters, I., De Maeyer, M., Wodak, S. J., Jenkins, J., Chiadmi, M. & Janin, J. (1992). *Biochemistry*, **31**, 5459–5466.

Lavie, A., Allen, K. N., Petsko, G. A. & Ringe, D. (1994). *Biochemistry*, **33**, 5469–5480.

Lee, C. Y., Bagdasarian, M., Meng, M. H. & Zeikus, J. G. (1990). *J. Biol. Chem.* **265**, 19082–19090.

Leslie, A. G. W. & Powell, H. R. (2007). *Evolving Methods for Macromolecular Crystallography*, edited by R. J. Read & J. L. Sussman, pp. 41–51. Dordrecht: Springer.

Meilleur, F., Snell, E. H., van der Woerd, M. J., Judge, R. A. & Myles, D. A. A. (2006). *Eur. Biophys. J.* **35**, 601–609.
Myles, D. A. A., Bon, C., Langan, P., Cipriani, F., Castagna, J. C., Lehmann, M. S. & Wilkinson, C. (1997). *Physica B*, **241**, 1122–1130.
Snell, E. H., van der Woerd, M. J., Damon, M., Judge, R. A., Myles, D. A. A. & Meilleur, F. (2006). *Eur. Biophys. J.* **35**, 621–632.
Terwilliger, T. C., Adams, P. D., Moriarty, N. W. & Cohn, J. D. (2007). *Acta Cryst.* D**63**, 101–107.
Tilbeurgh, H. van, Jenkins, J., Chiadmi, M., Janin, J., Wodak, S. J., Mrabet, N. T. & Lambeir, A. M. (1992). *Biochemistry*, **31**, 5467–5471.
Whitaker, R. D., Cho, Y., Cha, J., Carrell, H. L., Glusker, J. P., Karplus, P. A. & Batt, C. A. (1995). *J. Biol. Chem.* **270**, 22895–22906.
Whitlow, M., Howard, A. J., Finzel, B. C., Poulos, T. L., Winborne, E. & Gilliland, G. L. (1991). *Proteins*, **9**, 153–173.
Winn, M. D. *et al.* (2011). *Acta Cryst.* D**67**, 235–242.